Argonne NATIONAL LABORATORY

ANL-06/51

Comparison of the Results of Short-Term Static Tests and Single-Pass Flow-Through Tests with LRM Glass

Chemical Engineering Division

About Argonne National Laboratory

Argonne is a U.S. Department of Energy laboratory managed by UChicago Argonne, LLC under contract DE-AC02-06CH11357. The Laboratory's main facility is outside Chicago, at 9700 South Cass Avenue, Argonne, Illinois 60439. For information about Argonne, see www.anl.gov.

Availability of This Report

This report is available, at no cost, at http://www.osti.gov/bridge. It is also available on paper to the U.S. Department of Energy and its contractors, for a processing fee, from:

U.S. Department of Energy
Office of Scientific and Technical Information
P.O. Box 62
Oak Ridge, TN 37831-0062
phone (865) 576-8401
fax (865) 576-5728
reports@adonis.osti.gov

ANL-06/51

ARGONNE NATIONAL LABORATORY
9700 South Cass Avenue
Argonne, Illinois 60439-4837

COMPARISON OF THE RESULTS OF SHORT-TERM STATIC TESTS AND SINGLE-PASS FLOW-THROUGH TESTS WITH LRM GLASS

W.L. Ebert

Chemical Engineering Division

August 2006

INTENTIONALLY LEFT BLANK

CONTENTS

TABLES

FIGURES

ACKNOWLEDGMENTS

Solution analyses by Yifen Tsai is greatly appreciated.

ABSTRACT

Static dissolution tests were conducted to measure the forward dissolution rate of LRM glass at 70 ºC and pH(RT) 11.7 ± 0.1 for comparison with the rate measured with single-pass flow-through (SPFT) tests in an interlaboratory study (ILS). The static tests were conducted with monolithic specimens having known geometric surface areas, whereas the SPFT tests were conducted with crushed glass that had an uncertain specific surface area. The error in the specific surface area of the crushed glass used in the SPFT tests, which was calculated by modeling the particles as spheres, was assessed based on the difference in the forward dissolution rates measured with the two test methods. Three series of static tests were conducted at 70 ºC following ASTM standard test method C1220 using specimens with surfaces polished to 600, 800, and 1200 grit and a leachant solution having the same composition as that used in the ILS. Regression of the combined results of the static tests to the affinity-based glass dissolution model gives a forward rate of 1.67 g/(m^2d). The mean value of the forward rate from the SPFT tests was 1.64 g/(m^2d) with an extended uncertainty of 1.90 g/(m^2d). This indicates that the calculated surface area for the crushed glass used in the SPFT tests is less than 2% higher than the actual surface area, which is well within the experimental uncertainties of measuring the forward dissolution rate using each test method. These results indicate that the geometric surface area of crushed glass calculated based on the size of the sieves used to isolate the fraction used in a test is reliable. In addition, the C1220 test method provides a means for measuring the forward dissolution rate of borosilicate glasses that is faster, easier, and more economical than the SPFT test method.

1. INTRODUCTION

A series of glass dissolution tests was conducted following the American Society for Testing and Materials (ASTM)-International standard method C1220 to address the uncertainty in the surface area of crushed glass used in glass dissolution tests (ASTM 2006a). Crushed glass is commonly used in both static and dynamic tests to provide enough surface area that the amounts of dissolved glass components released into solution can be measured. An interlaboratory study (ILS) was recently performed to measure the precision of a single-pass flow-through (SPFT) test method conducted with crushed LRM glass[a] (Ebert 2006). Those tests provided a measure of the forward dissolution rate of LRM glass at 70 ºC in a LiOH/LiCl solution that imposed pH near 11.7 at room temperature (near 10 at 70 ºC). (The forward dissolution rate is the glass dissolution rate in the absence of solution feedback effects.) Whereas the precision of the measured rate was determined from the results of several laboratories, the accuracy of that rate depends on the accuracy of the specific surface area of the crushed glass that was used in the analysis. For the ILS, the specific surface area was calculated based on the sieve size fraction used in the test, as is commonly done for tests with crushed glass (e.g., ASTM 2006b). The primary objective of these C1220 tests is to estimate the uncertainty in the surface area term for crushed glass used in the ILS.

The ASTM C1220 test is a static test performed with a monolithic specimen having a known geometric surface area with quantifiable uncertainty. The C1220 tests were conducted with the same LRM glass in a LiOH/LiCl solution having the same composition that was used in the ILS and at the same temperature. The C1220 tests were conducted at a low glass surface-area-to-leachant volume (S/V) ratio to minimize solution feedback effects so that the glass dissolved at a rate near the forward rate. The difference between the rate measured with the C1220 tests using specimens with geometrically determined surface areas and the rate measured in the SPFT tests using crushed glass can be attributed primarily to (1) deviation in the rate measured in the C1220 tests due to solution feedback effects or (2) deviation in the surface area used in the SPFT tests due to the use of an inaccurate specific surface area. Another potential source of difference is the effect of the surface roughness of the monolithic samples used in the C1220 tests. The impact of that effect was evaluated by conducting series of C1220 tests with samples polished to different surface finishes. The effects of solution feedback in the C1220 tests can be judged by the effects of similar steady-state solution concentrations attained in the SPFT tests on the rates measured in those tests. The feedback effect in the C1220 tests can be taken into account using the affinity term in the rate equation for glass dissolution. The remaining deviation of the rates measured in SPFT and C1220 tests can be assigned to the difference between the true specific surface area of the crushed glass and the geometric approximation. This is because the specific rates measured in the SPFT and C1220 tests, in units of $g/(m^2d)$, are both the ratio of the rate at which a soluble component accumulates in solution (which is measured in the tests) and the surface area of the dissolving solid. In the C1220 tests, the greatest uncertainty is in the measured solution concentration. The uncertainty in the measured solution concentrations was similar in the SPFT tests, and dominated the propagated uncertainty in those rates (uncertainty in the surface area was neglected in the ILS analyses).

A second objective of these tests is to evaluate the use of the C1220 test method as an alternative to SPFT tests for measuring the forward glass dissolution rate. The SPFT test was designed to alleviate solution feedback effects on the dissolution rate (or control them at a desired level) by continuously flushing the dissolved components from the solution contacting the dissolving solid. The forward dissolution rate that

[a]The low-activity reference material (LRM) glass was developed for use as a standard test material for acceptance testing of low-activity waste (LAW) glasses produced at the Waste Treatment Plant at the DOE Hanford site (Ebert *et al.* 1998). The responses of the glass in several analytical and test methods considered for LAW glasses have been measured (Wolf *et al.* 1998), and LRM glass has been used in studies to evaluate the interlaboratory precision of glass composition analysis and product consistency tests (Ebert and Wolf 2000).

is measured in the absence of solution feedback effects is then used in a rate expression that includes a separate term for solution feedback to calculate the dissolution rate over long times; the value of the term used to take solution feedback into account must be determined with another test method. Although the C1220 test method allows dissolved components to accumulate in solution and solution feedback becomes significant even after very short test durations (depending on the test conditions that are used), a series of C1220 tests conducted for different times can be fitted with the rate expression for glass dissolution to determine both the forward rate and the solution feedback term. If the solution feedback term is known, it can be included in the analysis to determine the forward rate. Compared with the SPFT test method, the C1220 tests generate much less solution waste, require the analysis of fewer solutions, can be completed in less time, and have fewer testing artifacts. Artifacts in tests with crushed glass include the presence of high-energy sites due to fracturing (the impact of which can be avoided by excluding the eluent solution early in the test from the rate analysis) and the loss of surface area as the crushed particles dissolve during the test. More test material and more effort is required for the preparation of monolithic test specimens for the C1220 tests than is needed to prepare crushed glass samples, although the monolithic samples can be re-polished and used in other tests.

2. BACKGROUND

Crushed materials are generally used to provide a large surface area in laboratory tests conducted to measure dissolution behavior so that measurable solution concentrations can be attained in tests with slowly dissolving materials within reasonable test durations. For example, the Materials Characterization Center test number 3 (MCC-3) was designed to measure the maximum "solubility" of a material by using crushed material of various size fractions (Strachan *et al.* 1981). The product consistency test (PCT) for high-level radioactive waste glass is a variation of the MCC-3 test (ASTM 2006b) in which the amount of glass that dissolves within a fixed duration (7 days in PCT method A) is measured. The actual surface area provided by the crushed particles can be measured directly by gas adsorption or estimated based on the size fraction of sieved particles. Previous analyses comparing the reactivities measured in short-term static tests with crushed SYNROC and monolithic specimens indicated that the geometric surface area of the crushed material was about 50% too low and that an *ad hoc* roughness factor was needed to better match the results of tests with monolithic specimens (Oversby 1982). That study also showed that the calculated surface areas of various size fractions of crushed SYNROC gave better agreement than the surface areas measured by gas adsorption. This may indicate that the surface area accessible to the sorbing gas differs from the surface area accessible to water. For the purpose of modeling dissolution, it is the surface area available for reaction with water that is of interest. Other tests comparing the reactivities of crushed glass and monolithic specimens showed that the calculated geometric surface area of the crushed glass (–42 +60 mesh size fraction) was about 20% too high (Barkatt *et al.* 1981). However, those tests were conducted using a pulsed-flow method in which solution was periodically removed for analysis and replaced with fresh leachant so that solution feed back effects cannot be readily assessed or taken into account. It is likely that the rates measured with the crushed glass and monolithic specimens were both slowed by solution feedback, but to different extents.

The current study followed the approach used by Barkatt *et al.* (1981) and Oversby (1982), except the comparison was made using the forward dissolution rates measured using (1) an SPFT test method with crushed glass and (2) the ASTM C1220 static test method with monolithic specimens. The SPFT method was developed to avoid the buildup of dissolved glass components in the test solution, and is commonly used to measure the forward dissolution rate of borosilicate glasses (e.g., Knauss *et al.* 1990, McGrail *et al.* 1997). Recent results from an ILS to study the precision of the rate measured with an SPFT test are compared with new C1220 test results for the same glass at the same temperature and in the same leachant solution composition. The SPFT test method and ILS results are summarized in the following sections.

2.1 SUMMARY OF SPFT TEST METHOD

In an SPFT test, leachant is pumped through a reaction cell containing glass at a constant rate and the effluent solution exiting the cell is sampled periodically and analyzed for dissolved glass components. The glass dissolution rate can be calculated from the known flow rate and the steady-state concentration of a soluble glass component. Crushed glass is commonly used in SPFT tests to provide enough surface area that the amounts of dissolved glass components in the effluent solutions can be measured. Two complications of using crushed glass are that (1) high-energy points and edges of the fractured glass particles dissolve faster than the flatter facets and (2) the total surface area is uncertain because of the random sizes and shapes of the particles of crushed glass. In SPFT tests, the first issue can be addressed by allowing enough glass to dissolve that the high energy sites no longer contribute significantly to the measured rate. In this way, dissolved glass from high energy sites is flushed out of the system before samples are taken to measure the rate. In contrast, the dissolved glass from high energy sites accumulates in the test solution in static tests and is included in the analyses. If the samples used in different tests have nearly identical geometric surface areas and were prepared identically, the dissolution of high energy sites is expected to generate the same amounts of dissolved glass components in each test and not affect the rate.

The surface area of the crushed glass used in an SPFT test is usually calculated based on the size fraction of the crushed glass, as determined by the sizes of the sieves used to isolate the fraction (McGrail *et al.* 1997). This approach was used in the ILS SPFT tests (Ebert 2006), in which tests were conducted using the –100 to +200 mesh size fraction of crushed LRM glass. This is the fraction that passes through a 100 mesh size sieve (150 μm) but does not pass through a 200 mesh size sieve (75 μm). All particles were assumed to be spherical with a diameter equal to the arithmetic average of 100 and 200 mesh (U.S. designation) sieves, which is 112.5 μm. The specific surface area of the crushed glass was calculated to be 0.0210 m^2/g by using the density of the glass (which is 2516 kg/m^3). The glass surface area in each SPFT test was calculated as the product of the specific surface area and mass of glass used in that test. The relative uncertainty in the surface area (i.e., sample-to-sample variations due to weighing) was included in the overall precision of the SPFT test method in the ILS. The accuracy of the surface area was not known or taken into account in the analysis.

The composition of LRM glass was measured as part of an ILS conducted previously (Ebert and Wolf 2000). The consensus composition is summarized in Table 1. The LRM glass was formulated to represent low activity radioactive waste glasses to be made with Hanford tank wastes and includes surrogates for hazardous components (Ebert *et al.* 1998). The glass composition is also representative of

Table 1. LRM Glass Composition, Oxide Mass % ± Standard Deviation[a]

Oxide	Mass %	Oxide	Mass %	Oxide	Mass %
Al_2O_3	9.51 ± 0.34	K_2O	1.48 ± 0.49	NiO	0.19 ± 0.02
B_2O_3	7.85 ± 0.31	La_2O_3	0.02 ± nd[b]	P_2O_5	0.54 ± 0.07
CaO	0.54 ± 0.09	Li_2O	0.11 ± 0.03	PbO	0.10 ± 0.02
CdO	0.16 ± 0.02	MgO	0.10 ± 0.01	SO_3	0.30 ± 0.06
Cr_2O_3	0.19 ± 0.02	MnO	0.08 ± 0.01	SiO_2	54.20 ± 1.21
F	0.86 ± 0.11	MoO_3	0.10 ± nd	TiO_2	0.10 ± 0.01
Fe_2O_3	1.38 ± 0.18	Na_2O	20.03 ± 1.19	ZrO_2	0.93 ± 0.06

[a] Sum of mean concentrations = 98.77%.
[b] Standard deviation not determined from ILS.

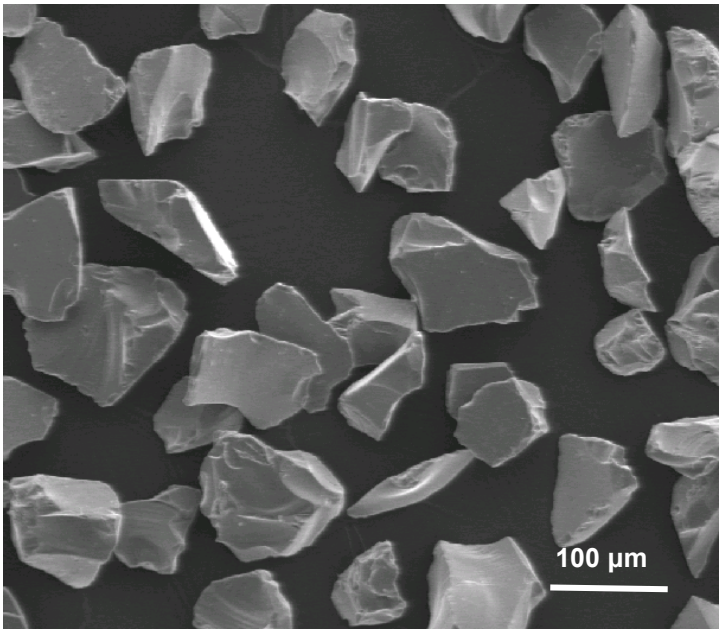

Fig. 1. Crushed LRM Glass in the –100 +200 Mesh Size Fraction. (Scale bar = 100 µm.)

high-level radioactive waste glasses, except the alkali metal content is higher than expected for most waste glasses. Figure 1 shows a scanning electron micrograph of crushed LRM glass used in the ILS. The particles are clearly not spherical (or cubic), but a 112.5-µm average dimension is a reasonable approximation of their average size (the scale bar in Fig. 1 is 100 µm). Although the calculated geometric surface area of crushed materials is sometimes multiplied by an *ad hoc* "roughness factor" having a value between 1 and 3 to take the irregularities in the particle shapes into account; this was not done for the ILS. The results of the current tests are used to evaluate the need for such a term.

2.2 SUMMARY OF SPFT TEST ILS RESULTS

In the SPFT test ILS, participants reacted crushed LRM glass in flowing LiCl/LiOH solution at several combinations of flow rate and mass of glass to generate different steady-state Si concentrations. The dissolution rate was calculated from the flow rate and steady-state Si concentration (see Appendix A). The dependence of the dissolution rate on the steady-state Si concentration was nearly linear at low Si concentrations, and the rate extrapolated to 0 concentration (the *y*-intercept) was taken as the forward dissolution rate. The results from 3 participants are shown in Figs. 2a – 2c. The three symbols in Fig. 2a denote three replicate tests. The dissolution rate decreases nearly linearly as the Si concentration increases to about 25 mg/L, at which point the rate does not change significantly as the Si concentration continues to increase. The concentration at which this occurs is estimated by the *x*-intercept of the lines in Figs. 2a and 2c, which are 32.5 mg/L and 21.5 mg/L, respectively.

The forward dissolution rates determined from the results of individual participants are summarized in Table 2. The results of all participants are combined in Figure 3a. Only the rates measured in tests with steady-state Si concentrations less than 10 mg/L were used to determine the consensus forward rate, and these are plotted in Figure 3b. Note also that the results F31-1, F31-2, F31-3, and F31-4 (plotted as F-1 in Fig. 3a) were excluded from the regression because these tests were conducted for very short durations

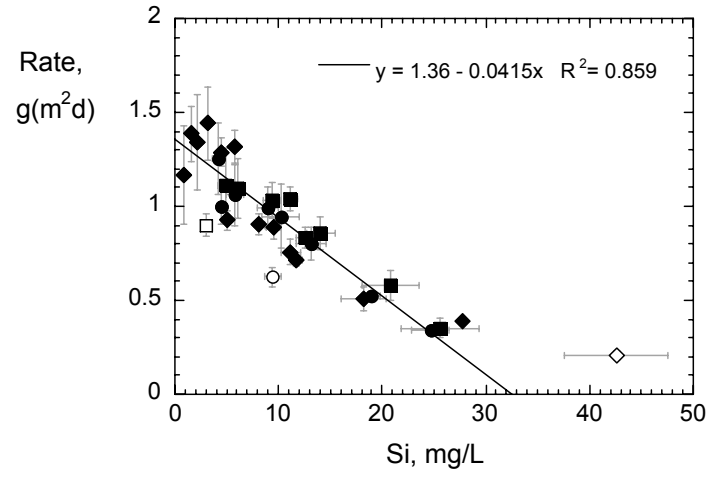

(a)

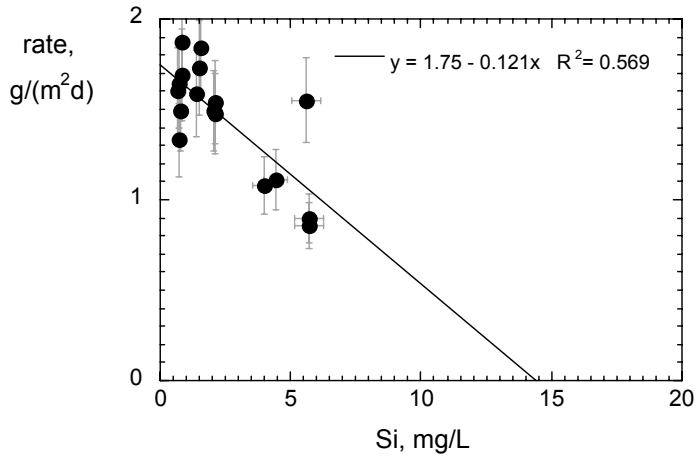

(b)

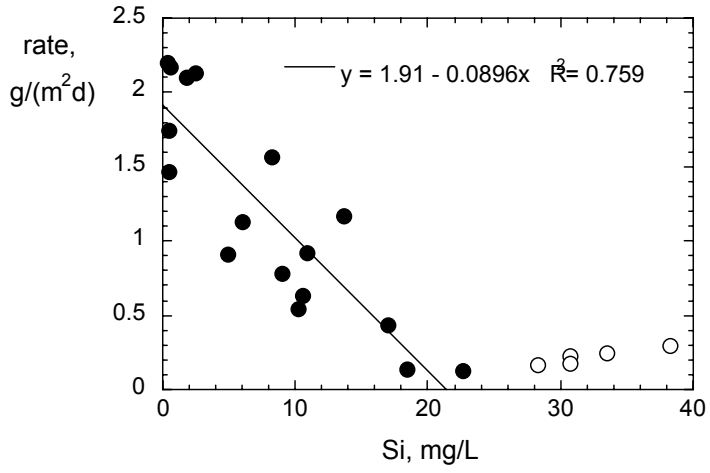

(c)

Fig. 2. Results of Individual SPFT Tests and Extrapolations for (a) Participant A, (b) Participant D, and (c) Participant G. (Open symbols were excluded from regression.)

Table 2. Summary of Forward Rates from ILS SPFT Tests

Participant	Forward rate, g/(m^{2}d)	Participant	Forward rate, g/(m^{2}d)
A1	1.25	F31-1	3.88
A2	1.29	F31-2	3.60
A3	1.35	F31-3	3.31
D	1.75	F31-4	1.36
E	1.14	G	1.91

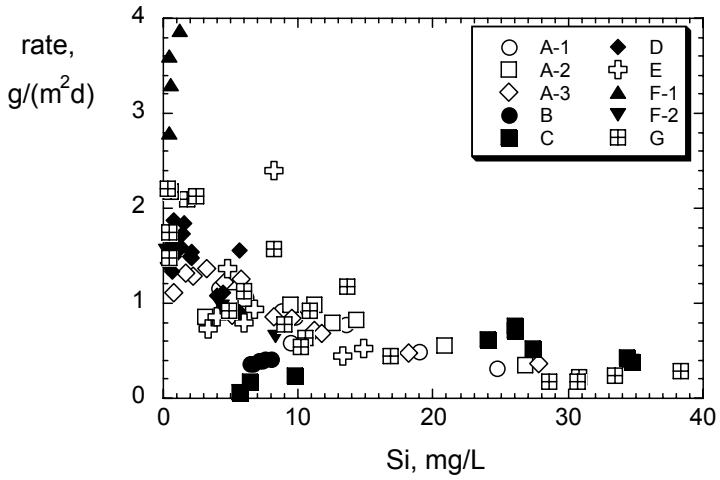

(a)

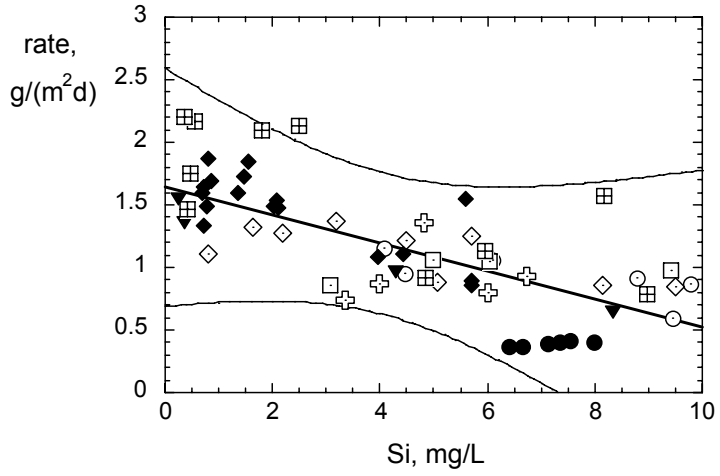

(b)

Fig. 3. (a) Combined Results from All Participants and (b) Subset of Results with Rates <2.3 g/(m^{2}d) and Steady-State Si Concentrations <10 mg/L. (All results plotted in (b) are included in the regression fit.)

(less than 1 day), and the measured rates were dominated by the initial transient dissolution of glass at high energy sites, such as sharp fracture edges (Ebert 2006). One rate measured by Participant E (Test LRM V: 2.40 g/(m^2d) at 8.24 mg/L) was excluded as an outlier. The linear fit and the uncertainty hyperbolae (from the estimated standard error in the regression) are shown in Figure 3b. From the combined results, the consensus average forward rate from the ILS SPFT tests is 1.64 g/(m^2d). The extended uncertainty (which is 2 times the estimated standard error in the *y*-intercept of the linear regression) was calculated to be 1.90 g/(m^2d). Note that this uncertainty quantifies the interlaboratory and intralaboratory, as well as experimental and analytical uncertainties.

It is worth noting that the scatter in the rates determined from tests with steady-state Si concentrations less than 10 mg/L is essentially the same at all Si concentrations. The results of a single test conducted under conditions that yield a very low Si steady-state concentration will carry this same uncertainty. The intra-laboratory uncertainty is similar to the inter-laboratory uncertainty. This is best seen with the results of Participants D and G at between 0.5 and 1.0 mg/L Si.

Finally, the composition of the LiOH/LiCl solution was specified in the ILS rather than the pH because it was anticipated that there would be less variation in the preparation of the leachant solution than in measuring its pH. This was indeed the case, where the measured pH values of the leachant solutions (at room temperature) ranged from about pH 10 – pH 12 for the 7 participants. Small differences in the pH are expected due to the sensitivity of the pH to the specific masses of LiOH, LiCl, and water used to make the solutions. However, the large discrepancies in measured leachant pH values seen in the ILS far exceed the expected range. These differences were treated as uncertainty in measuring the pH when determining the dissolution rate in the ILS, since the objective was to measure the precision with which the rate could be measured while maintaining constant reaction conditions (primarily the pH, temperature, and dissolved Si concentration). The effect of real variations in the pH values of the leachants used by different participants is included in the overall precision of the consensus rate determined in the ILS.

3. EXPERIMENTAL APPROACH

A large piece of LRM glass was prepared for use in the C1220 tests by melting crushed LRM glass (which was taken from the same source that was used in the ILS) in an alumina crucible at about 1200 ºC for about 2 hours. The furnace temperature was then lowered and the glass was allowed to cool to about 700 ºC in furnace, and then moved to an oven set at about 600 ºC and annealed several hours. That oven was then turned off and the glass allowed to cool slowly as the oven cooled. The resulting glass was cored using a diamond-coated coring bit, and the circumference of the core was polished to a final 600-grit finish. The core was then cut into wafers with a low-speed diamond saw and both faces of each wafer were polished to a final 600-grit finish. These specimens were used in the first series of tests. A second series of tests was conducted to study the effect of the surface finish. Rectangular specimens were cut from the remaining LRM glass and ground successively with 240-, 320-, 400-, 600-grit carborundum paper, and then to a final finish with 800-grit paper (both faces and the four edges). All coring, cutting, and polishing operation were performed manually using a metallurgical polishing wheel with water lubrication. The surface finishes of the sets of specimens prepared with each grit varied somewhat because they were polished manually (they were hand-held) and the grinding paper was not replaced for each sample and the edges of the specimens were slightly rounded. The finishes on the specimens used in each series were visually the same, and all samples had a mirror finish. The samples with a 600-grit finish had a few visible few scratches and the more finely polished samples had a slightly wavy appearance. The dimensions of each sample (diameter and thickness of the disc-shaped specimens and the side lengths and corner thicknesses of the rectangular specimens) were measured with a caliper to allow calculation of the geometric surface area.

The specimens that had been polished to an 800-grit finish and used in the second series of tests were later repolished for use in a third series of tests. They were initially polished with 600- and 800-grit paper to remove the surface layer of reacted glass formed in the initial test, and then polished to a final finish with 1200-grit paper. (No effort was made to track which specimens were used in each test within the second and third series.) The repolished specimens were dimensioned with calipers and assigned new specimen numbers. The third series of tests was conducted with leachant from the same source that was used in the second series.

Two batches of the 0.004 molal LiCl + 0.003 molal LiOH leachant solution were prepared for use (see Table 3). Batch I was used in the first series of tests and Batch II was used in the second and third series. The second series of tests (with 800-grit specimens) was conducted about 1 month after the first series was completed, and the third series was conducted about a week after the second series was completed.

Table 3. As-Batched Compositions of Leachant Solutions, in g

	$LiOH•H_2O$	$LiCl•H_2O$	Demineralized Water[a]
Batch I	0.2518	0.4835	1999.69
Batch II	0.2518	0.4828	2000.03

[a]Total mass solution.

All tests were conducted in 120-mL Teflon vessels with Teflon screens that held the specimens off the bottom of the vessel (Savillex Corporation Digestion Vessel 571B and Screen 465C). All tests were conducted in the same convection oven that was set at 70 ºC; the oven temperature was checked with a NIST-traceable thermometer when the vessels were placed into the oven and when they were removed. The temperature remained constant at 70.0 ± 0.5 ºC. The amount of leachant required to attain an S/V ratio of 1.8 m^{-1} with the glass specimen used in each test was calculated based on the geometric surface area of the specimen. That amount of leachant was first added to the vessel (by mass) and then the specimen was added. The tests were assembled in this order to prevent air bubbles from sticking to the specimen, which is more likely to occur if the leachant is poured over the specimen. The vessel was sealed and weighed, then placed into the oven. The time and date were recorded. The vessels have a screw-top lid and special wrenches for tightening them. One blank test (without glass) was conducted with each test series for the longest duration. The blank test was used to measure the background concentrations of B, Na, and Si to evaluate the extent of glass dissolution and to measure the concentration of Li to track the consistency of the leachant solution. At the end of each test, the vessel was removed from the oven and allowed to cool briefly (about 1 hour) and then weighed. The vessel was opened and a small amount of test solution was discarded by decanting. This was done to rinse the side of the vessel, and served also to gently mix the solution. An aliquot of the test solution was then poured into a solution bottle and saved for analysis. The remaining test solution was discarded. The glass specimen was removed from the vessel, rinsed with demineralized water, and then placed into a labeled vial. The test solutions were analyzed for pH with a combination pH electrode, then acidified with a few drops of concentrated HNO_3. The solutions were analyzed for B, Li, Na, and Si with inductively coupled plasma mass spectrometry (ICP-MS). As was done in the ILS, the accumulation of Si in the test solution was used to determine the glass dissolution rate.

The glass specimens were cut in the shapes of right square cylinders for Series 1 and rectangular wafers for Series 2 and 3. The diameters and thicknesses of the cylindrical samples were each measured to the nearest 0.01 mm at diagonally opposite locations using a caliper. The lengths of the 4 sides and thicknesses of the 4 corners of the rectangular wafers were measured; the sides and corners were numbered clockwise from an arbitrary starting point for recording the measured dimensions. The sample shapes are shown schematically in Figure 4. The dimensions of the cylindrical samples were measured in

millimeters and the dimensions of the rectangular wafers were measured in inches for Series 2 and in millimeters for Series 3. The area of each cylindrical specimen was calculated from the larger of two measurements of the diameter the average of two thickness measurements. (The perimeters were slightly out of round due to polishing of the cores and the faces were slightly out of parallel due to cutting and polishing.) The area of a rectangular wafer was calculated using the product of the average lengths of opposite sides for the large faces, and the product of the average length of opposite sides (one set of sides is referred to as the length and the other set as the width for convenience) and the average of the corner thicknesses. This takes into account that the wafers were not perfectly rectangular and models them as parallelepipeds. The areas for samples used in Series 2 were calculated in square inches and then converted to square centimeters using the factor $(2.54)^2$ $cm^2/inch^2$. The measured dimensions and calculated areas are summarized in Table 4. The methodology and uncertainty in the calculated areas is addressed in more detail in Appendix B.

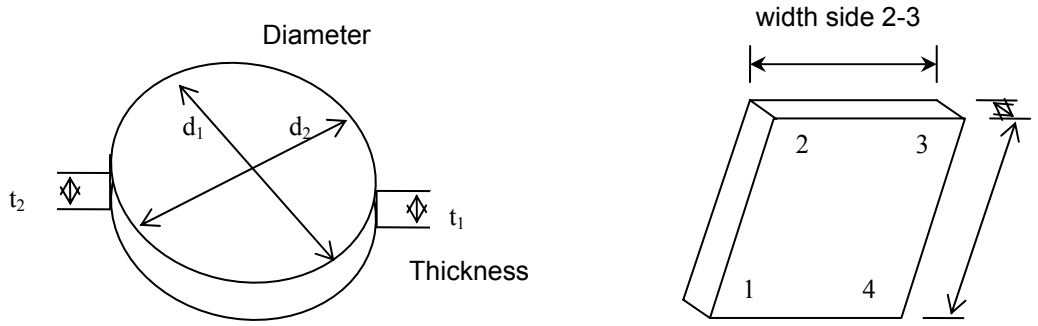

Fig. 4. Schematic Drawings of (a) Cylindrical and (b) Parallelepiped Specimens.

4. RESULTS

The test data for the C1220 tests are summarized in Table 5. The solution concentration of Li was measured to track the stability of the leachant solution. (The LRM glass contains only a small amount of Li.) Since the leachant solution contains LiOH to set the initial pH and LiCl to adjust the ionic strength, the Li concentration is expected to correlate with the solution pH. The measured Li concentrations are plotted against the pH values measured at room temperature in Figure 5. Uncertainty bars are drawn at ±10% for the Li concentrations and at ±0.05 pH units. The results are fairly tightly clustered for each test series (except for an anomalously high Li concentration in test LRM-23 in Series 2), but the Li concentration and pH within a series are not correlated. Overall, Series 1 has higher pH values than Series 2 or 3, but lower Li concentrations. Series 2 and 3 have similar pH values, but Series 2 has lower Li concentrations. The differences in the results of Series 2 and 3 are surprising because these test series were conducted with the same stock solution. The uniformly higher Li concentrations reported for Series 3 may be a symptom of analyzing the solutions with ICP-MS, which is not the best method for measuring low mass elements. From the as-batched solution compositions (see Table 3), the Li concentrations in Batches I and II are predicted to be 48.61 and 48.57 mg/L, respectively. The measured values of the test solutions from Series 1 and 2 are in good agreement with the expected concentrations, but the Li concentrations in the test solutions from Series 3 (include the blank test solution) are too high. However, the measured solution pH values for the solutions from Series 2 and 3 are in good agreement. About 57% of the Li is provided by $LiCl \cdot H_2O$, and it is possible that this was not totally dissolved when Series 1 and 2 tests were performed. The impact of glass dissolution on the Li concentration is negligible.

Table 4. Dimensions of Test Specimens

Cylindrical Specimens for Series 1 Tests (600-grit finish)							
	Diameter, mm		Thickness, mm			Surface Area, cm^2	
Sample Number	Larger value	Smaller value	1	2	Average		
LRM 1	9.16	9.50	1.71	1.40	1.555	1.88	
LRM 2	9.67	9.69	1.36	1.25	1.305	1.87	
LRM 3	9.67	9.71	1.62	1.62	1.620	1.98	
LRM 4	9.60	9.62	1.36	1.33	1.345	1.86	
LRM 5	9.67	9.73	1.39	1.40	1.395	1.91	
LRM 6	9.52	9.66	1.39	1.42	1.405	1.89	
LRM 7	9.22	9.53	1.38	1.35	1.365	1.84	
LRM 8	9.53	9.62	1.47	1.43	1.450	1.89	
LRM 9	9.30	9.45	1.30	1.28	1.290	1.79	
LRM 10	9.59	9.63	1.34	1.35	1.345	1.86	
LRM 11	9.36	9.40	1.44	1.43	1.435	1.81	
LRM 12	9.58	9.63	1.29	1.37	1.330	1.86	
LRM 13	9.63	9.65	1.59	1.54	1.565	1.94	

Rectangular Wafer Specimens for Series 2 Tests (800-grit finish)									
	Side length, inches				Corner thickness, inches				
Sample Number	Length 1-2	Width 2-3	Length 3-4	Width 4-1	1	2	3	4	Surface Area, cm^2
LRM 14	0.4025	0.2205	0.3950	0.2225	0.0270	0.0290	0.0275	0.0270	1.36
LRM 15	0.4030	0.3020	0.4100	0.3025	0.0260	0.0280	0.0275	0.0255	1.83
LRM 16	0.4035	0.2205	0.3975	0.2180	0.0270	0.0260	0.0280	0.0295	1.35
LRM 17	0.4080	0.3030	0.4020	0.3010	0.0285	0.0280	0.0285	0.0305	1.84
LRM 18	0.3965	0.2190	0.4025	0.2210	0.0260	0.0255	0.0235	0.0260	1.34
LRM 19	0.3920	0.2245	0.3990	0.2215	0.0290	0.0305	0.0290	0.0270	1.37
LRM 20	0.4010	0.2230	0.3935	0.2215	0.0255	0.0265	0.0265	0.0255	1.35
LRM 21	0.4085	0.3000	0.4015	0.3005	0.0260	0.0265	0.0280	0.0265	1.81
LRM 22	0.4120	0.3030	0.4035	0.3035	0.0285	0.0285	0.0280	0.0275	1.85
LRM 23	0.3175	0.2190	0.3130	0.2145	0.0285	0.0285	0.0285	0.0285	1.08

Rectangular Wafer Specimens for Series 3 Tests (1200-grit finish)									
	Side length, inches				Corner thickness, inches				
Sample Number	Length 1-2	Width 2-3	Length 3-4	Width 4-1	1	2	3	4	Surface Area, cm^2
LRM 24	10.12	5.59	9.91	5.53	0.59	0.62	0.63	0.57	1.30
LRM 25	10.12	5.63	9.98	5.55	0.62	0.63	0.64	0.65	1.32
LRM 26	10.00	5.56	10.17	5.52	0.70	0.69	0.63	0.64	1.33
LRM 27	10.37	7.64	10.17	7.66	0.64	0.67	0.71	0.60	1.81
LRM 28	10.10	5.61	9.93	5.69	0.68	0.66	0.69	0.72	1.35
LRM 29	10.42	7.61	10.17	7.66	0.71	0.70	0.68	0.71	1.82
LRM 30	10.08	5.53	10.05	5.62	0.62	0.66	0.65	0.63	1.32
LRM 31	10.28	7.57	10.17	7.57	0.64	0.64	0.60	0.65	1.77
LRM 32	7.98	5.44	7.92	5.51	0.69	0.70	0.67	0.68	1.05
LRM 33	10.18	5.52	9.97	5.60	0.55	0.58	0.59	0.62	1.30
LRM 34	9.99	5.62	10.11	5.55	0.58	0.64	0.60	0.56	1.31
LRM 35	10.05	5.57	10.18	5.54	0.69	0.67	0.66	0.66	1.33

Table 5. Test Data and Results for Short-Term Static Tests with LRM Glass

Test Number	Surface Area, cm^2	Leachant Mass, g	S/V, m^{-1}	Reaction Time, d	pH(24ºC)	Concentration, mg/L				NL(Si) g/m^2
						Li	B	Na	Si	
Series 1: Specimens with a 600 grit finish; Leachant Batch 1										
LRM 1	1.88	104.54	1.80	0.55	11.77	48.0	0.065	0.591	0.808	1.71
LRM 2	1.87	104.01	1.80	0.55	11.78	47.3	0.058	0.448	0.789	1.67
LRM 3	1.98	109.71	1.80	0.97	11.80	47.4	0.079	0.640	1.11	2.37
LRM 4	1.86	103.33	1.80	0.97	11.82	48.0	0.082	0.696	1.19	2.55
LRM 5	1.91	106.29	1.80	1.53	11.78	48.1	0.104	0.893	1.56	3.36
LRM 6	1.89	105.11	1.80	3.92	11.78	44.6	0.222	1.680	2.96	6.43
LRM 7	1.84	101.97	1.80	1.97	11.79	47.4	0.149	1.54	2.06	4.46
LRM 8	1.89	105.11	1.80	2.54	11.78	43.5	0.162	1.20	2.08	4.50
LRM 9	1.79	99.20	1.80	3.00	11.80	43.8	0.206	1.96	2.64	5.73
LRM 10	1.86	103.53	1.80	3.56	11.78	43.9	0.212	1.66	2.83	6.14
LRM 11	1.81	100.64	1.80	5.35	11.78	43.9	0.308	2.51	3.31	7.20
LRM 12	1.86	103.28	1.80	6.36	11.77	46.4	0.405	2.64	4.68	10.2
LRM 13	1.94	107.62	1.80	7.35	11.78	43.4	0.385	2.72	4.69	10.2
blank	—	104.41	—	7.35	11.82	47.4	0.021	0.028	0.029	—
Series 2: Specimens with a 800 grit finish; Leachant Batch 2										
LRM 14	1.36	75.60	1.80	0.59	11.58	50.4	0.0428	0.325	0.658	1.42
LRM 15	1.83	101.67	1.80	0.59	11.60	50.5	0.0356	0.334	0.513	1.10
LRM 16	1.35	75.22	1.80	1.03	11.60	50.4	0.0631	0.524	0.899	1.95
LRM 17	1.84	102.31	1.80	1.03	11.62	51.6	0.0549	0.418	0.859	1.86
LRM 18	1.34	74.22	1.80	2.02	11.61	51.5	0.112	0.996	1.700	3.70
LRM 19	1.37	76.03	1.80	2.98	11.62	49.2	0.154	1.25	2.14	4.67
LRM 20	1.35	74.84	1.80	5.68	11.61	49.5	0.285	2.42	4.22	9.23
LRM 21	1.81	100.69	1.80	5.02	11.59	49.4	0.242	1.83	3.19	6.97
LRM 22	1.85	102.97	1.80	4.00	11.60	48.2	0.196	1.39	2.44	5.33
LRM 23	1.08	59.85	1.80	8.68	11.59	67.9	0.551	3.62	5.99	13.1
Blank2	—	74.13	—	8.68	11.57	49.7	0.049	0.038	0.012	—

Table 5. (cont.)

Test Number	Surface Area, cm^2	Leachant Mass, g	S/V, m^{-1}	Reaction Time, d	pH(24ºC)	Concentration, mg/L				NL(Si) g/m^2
						Li	B	Na	Si	
Series 3: Specimens with a 1200 grit finish; Leachant Batch 2										
LRM 24	1.30	72.30	1.80	0.53	11.62	55.2	0.0673	0.395	0.448	0.970
LRM 25	1.32	73.46	1.80	0.53	11.63	55.3	0.0628	0.385	0.424	0.917
LRM 26	1.33	73.62	1.80	1.00	11.53	55.8	0.0897	0.543	0.917	2.00
LRM 27	1.81	100.34	1.80	1.64	11.63	56.4	0.108	0.673	1.1	2.40
LRM 28	1.35	74.84	1.80	2.32	11.62	55.6	0.192	1.23	1.97	4.31
LRM 29	1.82	101.28	1.80	4.93	11.61	53.3	0.246	1.71	2.87	6.28
LRM 30	1.32	73.47	1.80	4.26	11.62	55.7	0.233	1.67	2.72	5.95
LRM 31	1.77	98.51	1.80	3.67	11.63	55.6	0.216	1.48	2.47	5.40
LRM 32	1.05	58.58	1.80	1.96	11.63	56.7	0.138	0.914	1.43	3.12
LRM 33	1.30	72.40	1.80	6.03	11.58	56.4	0.302	2.36	3.86	8.45
LRM 34	1.31	72.70	1.80	6.94	11.55	56.0	0.327	2.57	4.26	9.33
LRM 35	1.33	74.10	1.80	7.93	11.52	55.9	0.375	2.94	4.88	10.69
Blank3	—	31.53	—	4.93	11.59	54.9	0.0548	0.084	<0.006	—

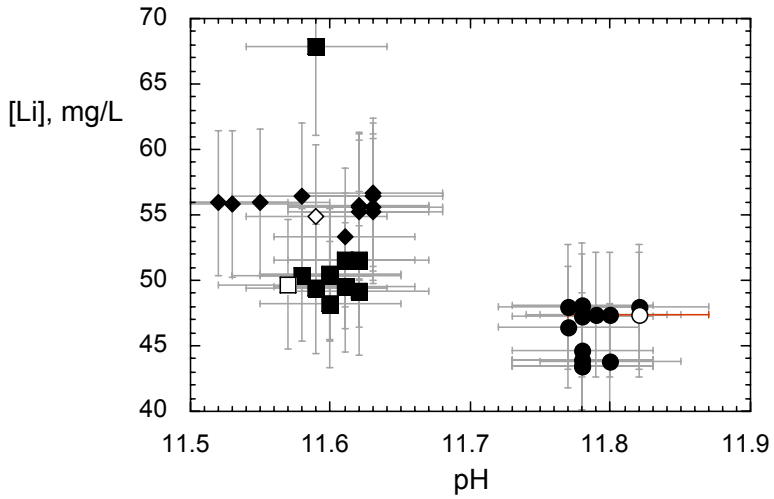

Fig. 5. Correlation between Li Concentration and pH (at room temperature). Series 1 with 600-grit finish (●), Series 2 with 800-grit finish (■), and Series 3 with 1200-grit finish (◆). Blank tests shown with open symbols.

The glass contains about 290 times more Na than Li, and the highest Na concentration attained in a test was 3.62 mg/L (LRM 23 in Series 2 see below). The releases of Li and Na are expected to be congruent under these test conditions, so that the highest contribution to the Li concentration due to glass dissolution is expected to be 0.012 mg/L.

The concentrations of B, Na, and Si were measured to track dissolution of the glass. The release of Si was used to determine the glass dissolution rate the ILS SPFT tests, and the Si release was used to determine the rate in the C1220 tests. The normalized elemental mass loss values were calculated to take into account the exact S/V ratio used in each test and the concentration of Si in the glass. The normalized elemental mass losses based on the amounts of Si measured in the test solutions will be used in subsequent calculations of the dissolution rate. It is calculated by using Equation 1.

$$NL(Si) = \frac{C(Si) - C^{o}(Si)}{S/V \bullet f(Si)}, \qquad (1)$$

where *NL(Si)* is the normalized mass loss based on Si, *C(Si)* is the Si concentration in the test solution, $C^{o}(Si)$ is the Si concentration in the blank test solution, and *f(Si)* is the mass fraction of Si in the glass—*f(Si)* = 0.2533. The values of NL(Si) and the pH (measured at room temperature) are plotted against the test duration in Figure 6. Uncertainty bars are drawn at ±11% of the NL(Si) values for all tests based on the propagated analytical uncertainties in test performance and solution analysis (see Appendix B) and at ±0.05 pH units. The solution pH values are constant in tests with specimens having 600- and 800-grit finishes, but decrease slightly with time in tests with specimens having 1200-grit finishes. The solution pH is slightly higher in the tests with specimens having 600-grit finish. As a first approximation, the dissolution rates are estimated by linear fits. The equations of the linear regression fits to NL(Si) are shown on the plots in Figure 6, and the dissolution rates are given by the slopes: 1.27 g/(m^2d) for specimens with a 600-grit finish, 1.44 g/(m^2d) for specimens with a 800-grit finish, and 1.28 g/(m^2d) for specimens with a 1200-grit finish.

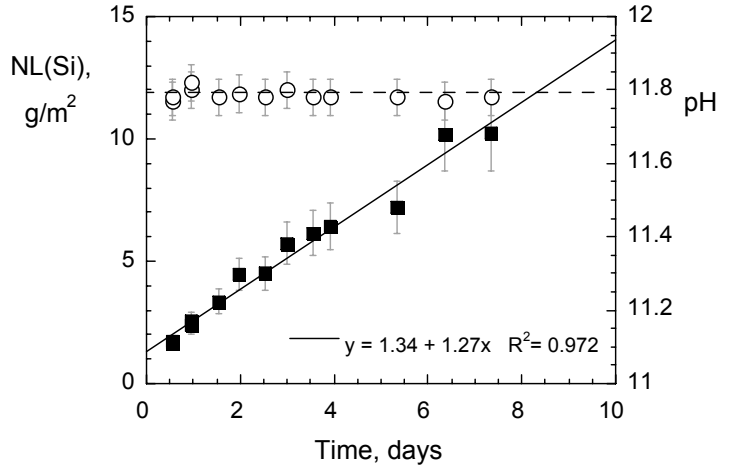

(a)

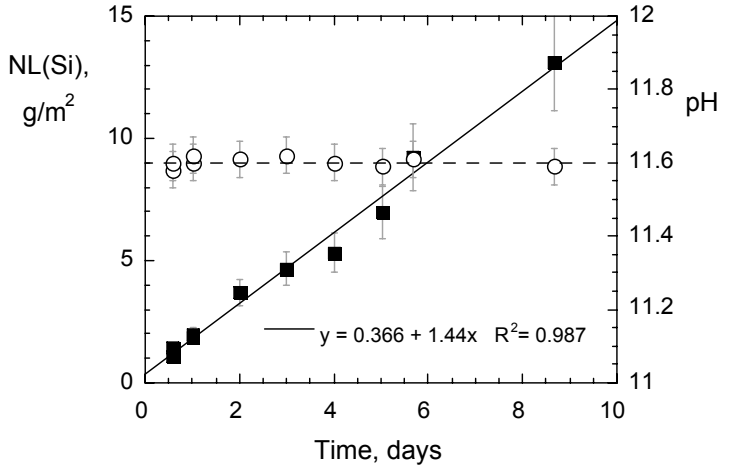

(b)

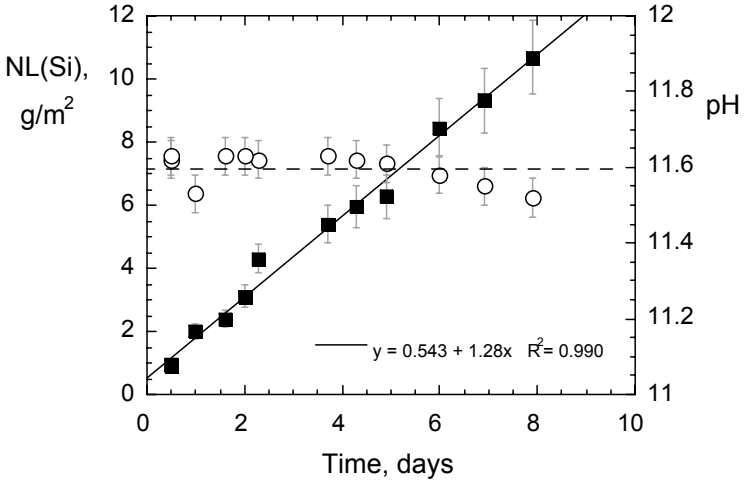

(c)

Fig. 6. Measured pH (O) and NL(Si) (■) for C1220 Tests with Monolithic Specimens Polished to (a) 600 Grit, (b) 800 Grit, and (c) 1200 Grit Finish.

Although the slightly higher pH values attained in the Series 1 tests are expected to increase the dissolution rate slightly, this series has the lowest rate determined with a linear fit. The average dissolution rate of the three test series is 1.34 g/(m^2d) with a standard deviation of 0.09 g/(m^2d) and a relative standard deviation of 6.5%. Note that all regressions have positive *y*-intercept values. This may indicate that the assigned background Si concentrations (from the blank tests conducted in each set of tests) are in error or may be due to the transient rapid dissolution of high-energy surface features that occurs in each test. Specimens prepared to have the same surface finish are expected to have similar amounts of glass in high-energy sites, so the effect is expected to increase the NL(Si) values of all tests in a series by a similar amount. Series 1 conducted with specimens having the roughest surface finish (600-grit) has the highest *y*-intercept. The fits of results of tests with 800- and 1200-grit finishes have similar *y*-intercepts. Another likely cause of the positive *y*-intercept is the effect of the chemical affinity on the dissolution rate: the dissolution rate slows with time and the data have a negative curvature. Fitting these data linearly leads to a positive *y*-intercept as a consequence of ignoring the curvature. That is, the linear regression underestimates the rate at short times and overestimates the rate at long times.

5. DISCUSSION

In static tests, the Si concentration increases with time as the glass dissolves and solution feedback becomes more important. The significance of solution feedback on the dissolution rate in the static tests can be assessed based on the dissolution rates determined in SPFT tests that attained different steady-state Si concentrations. As shown in Figure 3b, the dissolution rate in the SPFT tests varied nearly linearly with the steady-state Si concentration for values less than 10 mg/L. The solution concentrations attained in most of the C1220 static tests are less than 5 mg/L. From the SPFT results, the dissolution rate in a solution with 5 mg/L Si is about 1.1 g/(m^2d), which is about 67% of the consensus forward rate of 1.64 g/(m^2d). Therefore, the Si buildup in the static tests has a significant effect on the dissolution rate, and the effect increases with the test duration. While this is not obvious in the individual test series because of scatter in the results, a very slight negative trend can be seen when the results of the three series of C1220 tests are plotted together (this is most noticeable at short times), as in Figure 7. Linear regression of the *combined* results gives a rate of 1.32 g/(m^2d). The estimated standard error in the regressed slope of the combined results is 0.51 g/(m^2d), and the regression coefficient is $R^2 = 0.969$. This includes both the feedback effect of dissolved Si and effect of the different surface finishes.

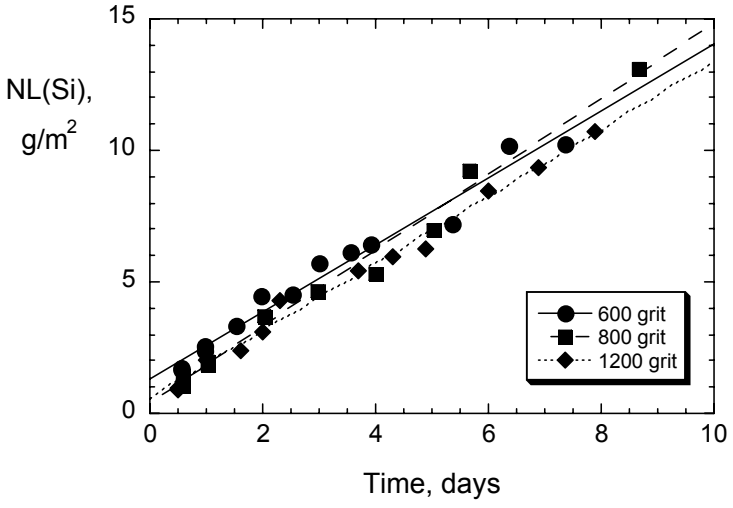

Fig.e 7. Plot of NL(Si) vs. Reaction Time for C1220 Tests.

5.1 SOLUTION FEEDBACK EFFECTS

The effect of solution feedback can be taken into account by regressing the combined test results with an expression that includes that effect. The equation to calculate the dissolution rate of a borosilicate glass is

$$rate = k_0 \bullet 10^{\eta \bullet pH} \bullet \exp\left(-E_a \big/ RT\right) \bullet \left(1 - \frac{Si}{K}\right), \tag{2}$$

where k_0 is the intrinsic rate constant, η is the pH dependence, E_a is the temperature dependence, and K is a pseudo-equilibrium constant for the glass. In the case of a single glass composition and at a constant pH and temperature, the first three terms on the right hand side of the equation can be replaced by a single term, k_f, which is the forward rate under those pH and temperature conditions. From the C1220 test results, the integrated rate after any time t can be calculated from the amount of Si in solution as

$$rate = \frac{NL(Si)}{t}. \tag{3}$$

This gives the rate based on the cumulative amount of glass that has dissolved (actually, based on the cumulative amount of dissolved Si that has accumulated) over that time. Values of k_f and K can be determined by equating the two expressions at a particular time t

$$NL(Si) = k_f \bullet \left(1 - \frac{Si}{K}\right) \bullet t, \tag{4}$$

where Si is the Si concentration measured in the test after a reaction time t. Note that the linear fit of the C1220 results models the rate using Equation 4 with Si = 0. The combined set of C1220 test data is used to determine the values of k_f and K that minimize the sum of the residuals between the calculated and measured values of NL(Si) for all test durations. The results of tests at all durations and with all surface finishes were weighted equally in the regression. The optimized fit is obtained with k_f = 1.667 g/(m^{2}d) and K = 35.59 mg/L. The values of NL(Si) calculated with Equation 4 at the test durations using these values of k_f and K are plotted in Figure 8 as small circles. The calculated values represent the experimental results well and overlie the linear fit to the combined data set (which is shown by the solid line). The uncertainty in the regressed values was not determined, but is expected to be similar to the uncertainty in the linear regression of the same data. The correlation coefficient was calculated to by R^2 = 0.951, which is slightly lower than that calculated for the linear fit of the combined data set. The uncertainty bars for the test results are drawn at 11% based on the propagated uncertainty in NL(Si); the propagated uncertainties are discussed in Appendix B. The forward rate from this analysis is k_f = 1.667 g/(m^{2}d), which is shown by the dashed line in Figure 8. The test results fall below this line at reaction times beyond about 4 days, which corresponds to Si concentrations above about 3 mg/L. The forward rate is about 26% higher than the rate determined from linear regression of the test results, which is consistent with the amount of solution feedback that was expected. The C1220 rate is slightly higher than the consensus forward rate of 1.64 g/(m^{2}d) from the ILS SPFT tests, but well within the uncertainty range.

The value K = 35.59 mg/L ($K = 10^{-2.897}$ M H_4SiO_4) that was determined by regression of the C1220 tests is reasonable; most borosilicate waste glasses are modeled to have a Si saturation concentration (solubility limit) of 28 mg/L or higher ($K \geq 10^{-3}$ M H_4SiO_4). The value of K is better measured with tests designed to approach saturation rather than these C1220 tests or the SPFT tests, both of which were designed to remain far from saturation. Since the test results were regressed to both parameters,

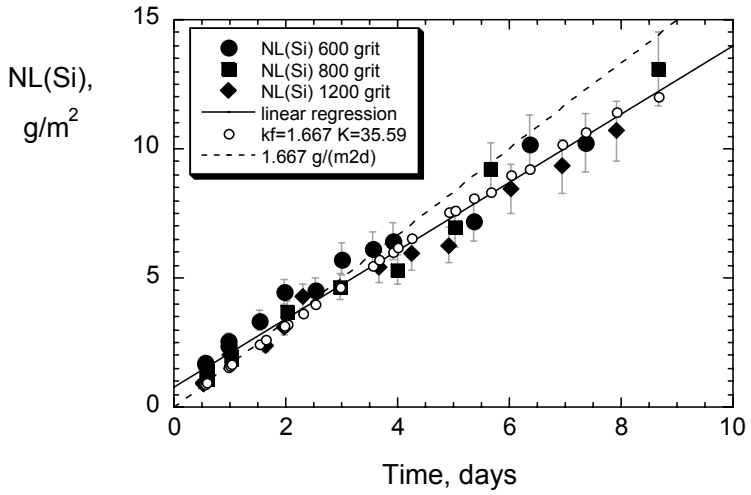

Fig. 8. Regression of Combined C1220 Test Rresults. Linear regression shown by solid line and regression to the equation $NL(Si) = k_f \bullet (1\text{-}Si/K) \bullet t$ using values $k_f = 1.667$ g/(m^{2}d) and $K = 35.59$ mg/L shown by small open circles.

uncertainty in the value of K is coupled with the uncertainty in the value of k_f. Recall that K is a pseudo-equilibrium constant used to model the glass.

The forward dissolution rate measured by either the C1220 or the SPFT test method is affected by the limitations to analyzing dilute solution concentrations. In both methods, measurable Si concentrations are needed to determine the rate, which means solution feedback effects are unavoidable. The dissolution rate in the absence of dissolved Si obviously cannot be measured directly. Nevertheless, many scientists conduct SPFT tests under conditions that attain very low Si concentrations and use that measured rate directly as the forward rate. That is, the feedback effects, which are small but not insignificant, are simply neglected. The scatter in the ILS SPFT test results seen at the lowest Si concentrations reveals the large uncertainty inherent in that approach. (The experimental uncertainty is probably exaggerated in the ILS results shown in Figure 3 because some of the participants had not performed SPFT tests prior to that study.) In the C1220 tests as used in this study, the accumulation of Si in solution after different test durations is used to determine the rate, but the results of tests at each duration can be "adjusted" to take the solution feedback effects into account by using Equation 4. In SPFT tests, different steady-state Si concentrations are needed to gauge the effect of dissolved Si on the rate in order to extrapolate the rate for a Si-free solution. The method used in the ILS also presumed a linear dependence of the rate on the Si concentration, whereas the fit of the C1220 results using Equation 4 does not. (The dependence of the rate measured in SPFT tests on the solution chemistry has been modeled to be non-linear with the Si concentration and to depend on other dissolved components. A linear extrapolation was selected for use in the ILS, in part, to facilitate calculation of the uncertainty.)

Both the C1220 tests and the SPFT tests are sensitive to the background Si concentration used in the rate calculations. Error in the background concentration does not affect the slope of the fit (provided the same background concentration is used for all tests), but it does affect the y-intercept. The linear fit to the C1220 results will not be affected, but the regression to Equation 4 will be affected. The rate calculated from the SPFT test results is also sensitive to uncertainty in the background concentration. The y-intercept used in the SPFT test method will be more sensitive to the background concentration than will the slope that is used in the C1220 method.

5.2 SPECIFIC SURFACE AREA OF CRUSHED LRM GLASS

The primary objective of the C1220 tests was to determine the specific surface area for crushed glass used in the SPFT tests. If the true dissolution rate is 1.67 g/(m^2d), then the consensus rate of 1.64 g/(m^2d) calculated in the ILS is about 1.5% too low, which means the specific surface area of 0.0210 m^2/g used in the ILS is 1.5% too high and the specific surface area should be 0.0207 m^2/g. The small difference is well within testing uncertainty. In the ILS, the uncertainty in the actual surface area was presumed to be on the order of a factor of 2 (i.e., ±100%). These results with LRM glass indicate that the uncertainty is far lower, and that the geometric surface area that is calculated by modeling the crushed glass as spheres with a diameter equal to the arithmetic average of the sieve sizes provides an adequate estimate of the true surface area. This result is relevant to static tests conducted with crushed glass, most importantly the product consistency test (PCT) (ASTM 2006b) that is used as an acceptance criterion for high-level radioactive waste glass. Previous analyses comparing the results of static tests with crushed glass and monolithic specimens indicated that the geometric surface area calculated for crushed materials was too low and that an *ad hoc* roughness factor was needed (Oversby 1982). Other tests showed the calculated geometric surface area was too high (Barkatt *et al.* 1981). It is likely that neither (1) the solution feedback effects in the tests with monoliths nor (2) the dissolution of high energy sites on the fractures surfaces were taken into full account in these tests, and that the forward dissolution rates were not used in either of those comparisons. Which of these has a greater effect will determine whether the calculated geometric surface area appears to be too high or too low. From the present work, in which the forward dissolution rates were used in the comparison, artificially increasing or decreasing the specific surface area by using a roughness factor is not necessary.

Clearly, the specific surface area calculated for a particular size fraction of crushed glass is a representative average of a collection of particles having a wide range of individual surface areas (see Fig. 1), and a large number of particles must be averaged for the calculated total surface area to be valid. For the –100 +200 mesh size fraction of LRM glass, which has a density of 2.516 g/cm^3, there are about one-half million particles in 1 g of crushed glass. Most tests in the SPFT test ILS were conducted with 0.1 g of glass, although some were conducted with less than 0.01 g (Ebert 2006). The use of small amounts of sample in SPFT tests can reduce the amount of liquid waste generated during the test. However, the reliability of the specific surface area calculated based on the size fraction decreases as fewer particles are used, although it is not known how few particles are required for the effect to be measurable. It may be that the uncertainty in the measured mass will become significant before the number of particles does. In the ILS SPFT tests, the effect of the mass of crushed glass used in a test (the number of particles) was not deconvoluted from the effect of the solution flow rate. Four tests with less than 0.01 g of glass run by Participant G (as low as 0.00488 g) resulted in the 4 lowest steady-state Si concentrations (see Fig. 2c). The rates in 2 of the tests were higher than the extrapolated forward rate and the rates in 2 tests were lower. However, the range of rates (the uncertainty in the rates) was similar to the range in tests conducted with more glass that resulted in higher steady-state Si concentrations. This is interpreted to indicate that the geometrically calculated surface area is adequate for masses as low as 0.00488 g.

It is important to note that the initial dissolution of crushed glass is dominated by the dissolution of glass at high-energy sites such as along fracture ridges and points. Based on the ILS SPFT test results, glass at these sites dissolves at a rate that is about 3 times that of the bulk glass. This has a significant effect on the SPFT test results at early test times, and the effluent solution generated when high-energy sites dominate the test response should not be used to determine the steady-state Si concentration. The time required for the glass at high-energy sites to dissolve will depend on the durability of the glass and the test conditions (leachant flow rate, temperature, and pH). For LRM glass in the ILS, the glass at high-energy sites was dissolved away within a few hours. The monolithic specimens used in the C1220 tests do not have fracture surfaces, but may have a small number of high-energy sites, for example, along polishing

scratches. These can be assumed to be similar on all samples having the same polish and are included in the measured rate. The effect of fracture surfaces in static tests with crushed glass, such as the PCT, could be significant in short-duration tests with durable glasses, but is expected to be insignificant in most tests because the high-energy sites represent only a small fraction of the total amount of glass that dissolves in a PCT. The rate determined in the ILS SPFT tests was for dissolution after the glass at the high-energy sites had dissolved.

The dissolution of crushed glass will usually lead to a decrease in the total surface area. (It is also possible that the surface area could increase due to surface roughening.) The loss of surface area is commonly estimated by modeling the glass particles as shrinking spheres (e.g., McGrail *et al.* 1997). In this model, the final surface area of the reacted glass, S_f, is calculated using the expression

$$S_f = \left\{ \frac{6}{\rho \bullet d_o} \right\} \bullet m_o^{1/3} \bullet m_f^{2/3}, \tag{5}$$

where ρ is the density of the glass, d_o is the initial diameter of the glass particle, m_o is the initial mass of the sample, and m_f is the final mass of the sample, which can be calculated from the dissolution rate and reaction time. If a glass is dissolving at a constant rate, then the loss of surface area should lead to a decrease in the steady-state Si concentration over time and could result in an underestimation of the dissolution rate. The use of small particles should be avoided in SPFT tests for this reason. In the ILS SPFT tests, evidence of possible loss of surface area was seen in only a few tests conducted at high flow rates.

5.3 SURFACE FINISH OF MONOLITHIC SPECIMENS

The significance of the surface finish of monolithic specimens on the dissolution rate is obscured by the scatter in the test results, but it appears to be small. The effect can be estimated from linear regression of the combined results. The dissolution rate based on linear regression is 1.32 g/(m^2d) with an estimated standard error of 0.51 g/(m^2d). This relative uncertainty of about 39% includes contributions from testing uncertainty and failure to account for solution feedback effects, as well as surface finish effects. The propagated uncertainty for individual C1220 tests due to analytical measurements (sample dimensions, weights, and solution analysis) is typically about 11%. The effect of solution feedback was estimated earlier to be about 26% at the longest test duration based on the difference in the rates from linear regression and regression to Equation 4. The remaining 2% can be attributed to differences in the surface finishes. This small predicted effect is consistent with the small difference in rates seen in tests with different surface finishes (Figs. 5 and 6). This result is consistent with previous studies that showed small effects for surface finishes of 600 grit and finer (Buckwalter *et al.* 1982; Dussossoy *et al.* 1992).

5.4 USE OF C1220 TEST TO MEASURE FORWARD DISSOLUTION RATES

Finally, this comparison of the C1220 and SPFT test results not only indicates that the geometrically calculated surface area of crushed glass is accurate within testing uncertainties, but that the C1220 test method provides a convenient approach for measuring the forward dissolution rate of a borosilicate glass. The SPFT test method was designed to minimize changes to the chemistry of the test solution as the glass dissolves by continuously flushing the dissolved glass components from the system. The forward rates measured at very low Si concentrations are then used in a rate expression similar to Equation 2 (with a value of K that is determined by other tests) to calculate glass dissolution rates at higher Si concentrations. Use of the SPFT test method to measure forward dissolution rates requires that separate tests be conducted at different solution flow rates to measure the rate at several steady-state Si concentrations in

order to extrapolate the rate to the absence of dissolved Si. Several samplings of the effluent solution must be analyzed over a several-day period (usually less than 14 days) to verify that the system is at or near steady state. The uncertainty in the rate determined in the SPFT tests is dominated by the uncertainty in the measured Si concentration, which is typically only slightly higher than the Si concentration in the leachant. As seen in both SPFT and C1220 tests, feedback effects become non-negligible even at very low Si concentrations.

In the ILS SPFT tests, the rates measured in tests with steady-state Si concentrations that provided significant feedback were used to extrapolate the rate to a Si concentration of 0 mg/L. This approach reduced the impact of the uncertainties of the rates measured at very low Si concentrations on the determined forward rate, but the use of a linear extrapolation is an approximation, since the relationship between K and the solution composition is not known. The inclusion of only the Si concentration to determine K is also an approximation. A non-linear approach similar to that taken with these data should be possible, but would still be empirical. Several scoping tests are usually needed to determine the flow rate and amount of glass to use in the SPFT tests to generate steady-state Si concentrations that are high enough to measure but low enough to have only a small feedback effect on the glass dissolution rate. This points to an important drawback of the SPFT test method, especially tests with hazardous and radioactive materials, namely, the large volume of waste solution that is generated. For example, one of the tests in the ILS was conducted with 0.5 g of glass at flow rate of 1.4×10^{-2} g/s and attained a steady-state Si concentration of about 3.2 mg/L. From Figure 3b, the dissolution rate in this test was significantly lower than the forward rate. About 12 L of waste solution was generated by running that one test for 10 days! Additional tests (which would generate additional waste) would be required to determine the forward rate.

The C1220 method provides an attractive alternative to the SPFT test method. Although dissolved glass components accumulate over time in the static C1220 tests, the rate at which they accumulate and their effect on the rate can be minimized by using very low S/V ratios and short test durations, and then quantified by using Equation 4. For these tests with LRM glass, the effect of dissolved Si in any particular C1220 test can be estimated by comparison with the SPFT test results (i.e., the regression line in Fig. 3b). The effect of accumulating dissolved components on the test series is evaluated by regressing Equation 4 to the test data themselves. Only a small number of tests (e.g., 5 or 6) and analyses is needed to determine the dissolution rate, although a larger number of tests will reduce the uncertainty. The uncertainty in the measured solution concentration also dominates the uncertainty in the rate determined by using C1220 tests, but the impact of the concentration on the equation of the fitted curve is less than the impact on the y-intercept in the SPFT tests. This is due, in large part, to the uncertainty in the line (or curve) used to extrapolate the SPFT test results to a Si concentration of 0 mg/L. The C1220 results are fitted directly using the glass dissolution equation (Eq. 4), and provide values of both k_f and K. Whereas the value of k_f is applicable at a specific pH value and temperature, running test series at various pH and temperatures provides values for the model coefficients η and E_a needed to use Equation 1. (The value of K is expected to be independent of the pH and temperature.) A drawback to the C1220 method is that the preparation of monolithic specimens and measuring their dimensions requires more effort than preparing a sample of crushed glass, especially samples of highly radioactive glasses. Glasses must be annealed to allow test specimens to be cut and polished without cracking. Sample preparation in a glove box is fairly routine, though time-consuming. Nevertheless, the use C1220 tests will be more economical and practical than SPFT tests in many situations because less effort is required to conduct a series of C1220 tests and much less waste solution is generated.

6. CONCLUSIONS

The forward dissolution rate determined from the combined results of C1220 tests conducted with specimens polished to a 600-, 800-, or 1200-grit finish is 1.67 g/(m^2d) when the effects of solution feedback are taken into account. This rate is consistent with the forward rate measured in the ILS SPFT tests, which is 1.64 ± 1.90 (g/m^2d). The rate from the SPFT tests was calculated by assuming the specific surface area of the -100 +200 mesh size fraction of crushed glass used in the tests was 0.0120 m^2/g. The rates measured in the C1220 and SPFT tests are compared directly by assuming that the dissolution rate of LRM glass will be the same at the same pH and temperature when the dissolved Si concentrations are the same. This assumes that the effect of solution flow (erosion) on the dissolution rate in the SPFT tests is negligible. The difference in the rates was attributed to solution feedback effects in the C1220 tests and error in the specific surface area of the crushed glass in the SPFT tests. After adjusting the results of the C1220 tests to account for solution feedback by using the glass dissolution equation, it was determined that the adjusted specific surface area for the -100 +200 mesh size fraction of LRM glass is about 1.5% *lower* than the geometrically estimated area. The small difference in the surface area is less than the uncertainty in the determined rate. The results of tests with this size fraction of LRM glass indicate that the geometric surface area calculated based on the sieve size fraction provides an adequate estimate of the actual surface area within the range of typical testing uncertainties. Although this finding is relevant to static tests with crushed glass, such as the PCT, it is important to note that it applies to crushed glass after the high-energy sites (e.g., along fracture edges) have been dissolved. A simple linear regression of short-term C1220 tests neglects solution feedback effects, which are likely to be significant for most waste glasses, and underestimates the forward dissolution rate. The forward dissolution rate is better estimated by fitting the C1220 results to the rate equation (see Eq. 4) and regressing both k_f and K.

REFERENCES

ASTM 2006a. *Test Method for Static Leaching of Monolithic Waste Forms for Disposal of Radioactive Waste*. American Society for Testing and Materials-International Standard C1220, Annual Book of ASTM Standards, Vol 12.01, West Conshohocken, PA.

ASTM 2006b. *Standard Test Methods for Determining Chemical Durability of Nuclear Waste Glasses: The Product Consistency Test (PCT)*. American Society for Testing and Materials-International Standard C1285, Annual Book of ASTM Standards Vol. 12.01, American Society for Testing and Materials, West Conshohocken, PA.

Barkatt, Aa., Barkatt, A., Pehrsson, P.E., Szoke, P., and Macedo, P.B. 1981. "Static and Dynamic Tests for the Chemical Durability of Nuclear Waste Glass," *Nuclear and Chemical Waste Management, 2*, 151-164.

Buckwalter, C.Q., Pederson, L.R., and McVay, G.L. 1982. "The Effects of Surface Area to Solution Volume Ratio and Surface Roughness on Glass Leaching." *Journal of Non-Crystalline Solids*, 49, 397-412.

Dussossoy, J.L, Dubois, C., Vernaz, E., and Chambaudet, A. 1992. "Effect of Surface Finish on Nuclear Glass Dissolution Rate," Material Research Society Symposium Proceedings, 257, 109-115.

Ebert, W.L. 2006. Interlaboratory Study of the Reproducibility of the Single-Pass Flow-Through Test Method: Measuring the Dissolution Rate of LRM Glass at 70 C and pH 10. Argonne National Laboratory report ANL-05/33.

Ebert, W.L., and Wolf, S.F., 2000. "An Interlaboratory Study of a Standard Glass for Acceptance Testing of Low-Activity Waste Glass." *Journal of Nuclear Materials, 282*, 112-124.

Ebert, W.L., Strachan, D.M., and Wolf, S.F. 1998. *Formulation of a Candidate Glass for use as an Acceptance Test Standard Material*. Argonne National Laboratory report ANL-98/10.

Knauss, K.G., Bourcier, W.L., McKeegan, K.D., Merzbacher, C.I., Nguyen, S.N., Ryerson, F.J., Smith, D.K., and Weed, H.C. 1990. "Dissolution Kinetics of a Simple Analogue Nuclear Waste Glass as a Function of pH, Time, and Temperature." *Material Research Society Symposium Proceedings*, 176, 371-381.

McGrail, B.P., Ebert, W.L., Bakel, A.J., and Peeler, D.K. 1997. "Measurement of Kinetic Rate Law Parameters on a Na-Ca-Al Borosilicate Glass for Low-Activity Waste." *Journal of Nuclear Materials,* 249, 175-189.

Oversby, V.M. 1982. *Leach Testing of Waste Forms: Interrelationship of ISO- and MCC- Type Tests*, UCRL 87621.

Strachan, D.M., Barnes, B.O., and Turcotte, R.P.. 1981. "Standard Leach Tests for Nuclear Waste Materials." *Material Research Society Symposium Proceedings*, 3, 347–354

Wolf, S.F.; Ebert, W.L.; Luo, J.S.; and Strachan, D.M. 1998. *A Data Base and a Standard Material for Use in Acceptance Testing of Low-Activity Waste Products*. Argonne National Laboratory report ANL-98/9.

APPENDIX A. GLASS DISSOLUTION RATE EQUATION

The rate expression commonly used to model borosilicate glass dissolution is given in Equation A-1:

$$rate = k_0 \bullet 10^{\eta pH} \bullet \exp\left(\frac{-E_a}{RT}\right) \bullet \left(1 - \frac{Q}{K}\right), \quad \text{(A-1)}$$

where

$rate$ = specific dissolution rate, g/(m^{2}d),
k_0 = intrinsic rate constant, g/(m^{2}d),
η = pH dependence, unitless,
E_a = activation energy, kJ/mol,
R = gas constant, kJ/(mol K),
Q = ion activity product of the solution, M, and
K = pseudo-equilibrium constant for the glass, M.

The term $\left(1 - \frac{Q}{K}\right)$ accounts for solution feedback, where Q/K gives the ratio of the solution concentration to that of an apparent saturation solution. Since glass is thermodynamically unstable, the solution can never become saturated and a true equilibrium constant does not exist. Instead, the conditions under which the dissolution rates are immeasurably low are modeled as saturation conditions, and the solution concentrations are represented by K. The SPFT test method can be used to provide a measure of the dissolution rates at different values of pH, temperature, and Q/K that are controlled during the test. In most cases, test conditions are selected to maintain dilute solutions in which $Q<<K$. For the ILS, participants were asked to conduct tests under several conditions to generate a range of Q/K values at fixed pH and temperature to measure the rate at various values of Q/K.

The dissolution rate is determined experimentally from the amount of a soluble component i released into solution from a known exposed surface area over a known duration, where the mass fraction of component i in the glass is also known. The rate expression is

$$rate = \frac{m(i)}{S^\circ \bullet f(i) \bullet t}, \quad \text{(A-2)}$$

where

$m(i)$ = mass of element i released from glass, g,
S^o = initial surface area of the crushed glass, m^2,
$f(i)$ = mass fraction of element i in the original glass, unitless, and
t = test duration, s.

The term $f(i)$ relates the mass of element i that is released to the mass of glass that has dissolved. Expressing the amount of the released component i as a concentration gives

$$rate = \frac{C(i) \bullet V}{S^\circ \bullet f(i) \bullet t}, \quad \text{(A-3)}$$

where

$C(i)$ = concentration of element i released from glass, g/m^3, and
V = volume of solution, m^3.

The concentration of i due to glass dissolution is the measured steady-state concentration $C^{ss}(i)$ minus the concentration of i present in the leachant $C^o(i)$.

$$C(i) = C^{ss}(i) - C°(i) \tag{A-4}$$

Under static test conditions, Equation A-3 can be written as

$$rate = \frac{NL(i)}{t} = NR(i) \ . \tag{A-5}$$

Under flowing conditions and at steady state, the term *V/t* is defined as the volumetric flow rate *F*. Substituting

$$rate = \frac{[C^{ss}(i) - C°(i)] \bullet F}{S° \bullet f(i)} = NR(i)\,, \tag{A-6}$$

where

NR(i) = normalized dissolution rate, g/(m^{2}d),
$C^{ss}(i)$ = steady-state concentration of Si in effluent, mg/L,
$C°(i)$ = concentration of element *i* in control test, mg/L,
F = leachant volumetric flow rate, m^3/s,
$S°$ = initial surface area of the crushed glass, m^2, and
f(i) = mass fraction of element *i* in the original glass.

In static tests, the forward dissolution rate is determined as the slope of a plot of NL(i) vs. *t*. In SPFT tests, the forward dissolution rate is determined as the *y*-intercept of a plot of *rate* vs. $C^{ss}(Si)$.

APPENDIX B. PROPAGATION OF ERRORS

The uncertainties in calculated values were estimated from the measured values using the propagation of errors method. For a property P that is a function of measured values x_1, x_2, x_3, etc., the probable error associated with P (Q_P) can be expressed in terms of the probable error in the means of the measured values (q_1, q_2, q_3, etc.) as

$$Q_p^{\,2} = \left(\frac{\partial P}{\partial x_1}\right)^2 \bullet q_1^{\,2} + \left(\frac{\partial P}{\partial x_2}\right)^2 \bullet q_2^{\,2} + \left(\frac{\partial P}{\partial x_3}\right)^2 \bullet q_3^{\,2} + \ldots \qquad \text{(B-1)}$$

The estimated uncertainties for measured and calculated values are listed below.

B.1 ELEMENTAL MASS FRACTION

The uncertainty in the elemental mass fraction *f*(*i*) is due to uncertainty in the mass of glass dissolved for analysis, the volume of the solution used to dissolve the glass, and the analysis of the solution. The uncertainty in the values of *f(i)* are estimated using the standard deviation of results for LRM glass analysis in the ILS. From Table 1, the SiO_2 content is 54.20 ± 1.21 mass% and the corresponding values for elemental Si are 25.327 ± 0.565 mass%. The value of *f(Si)* used for calculations in this report is 0.2533 with an uncertainty of 0.0057.

B.2 GLASS SURFACE AREA

The uncertainty in the surface area of monolithic specimens is due to uncertainties in the measured dimensions and using the geometric surface area. Any additional surface area due to surface roughness was neglected.

B.2.1 Circular Specimens

The area of each disk-shaped specimen was calculated using the larger of two measurements of the diameter (*d*) and the average of two measurements of the thickness (*h*) by assuming the disk was a right circular cylinder (see Fig. 4). The surface area was calculated as:

$$area = \frac{\pi\, d^2}{2} + \pi \bullet d \bullet h\,. \qquad \text{(B-2)}$$

Applying Equation B-1 to the area calculated with Equation B-2 gives, with $\partial S/\partial d = \pi h + \pi d$ and $\partial S/\partial h = \pi d$,

$$Q_A^{\,2} = (\pi \bullet h + \pi \bullet d)^2 \bullet q_d^{\,2} + (\pi \bullet d)^2 \bullet q_h^{\,2}\,. \qquad \text{(B-3)}$$

All dimensions were measured to ±0.0005 inches (0.013 mm), so that $q_d = q_h$ 0.013 mm. For example, the larger of the two diameters measured for specimen LRM 1 is 9.50 mm and the average of the two thicknesses is 1.555 mm. Substituting these values into Eq. B-3 gives

$$Q_A^{\,2} = (\pi \bullet 1.555 + \pi \bullet 9.50)^2 \bullet (0.00013)^2 + (\pi \bullet 9.50)^2 \bullet (0.00013)^2 = 0.3544\ mm^2 \qquad \text{(B-4)}$$

so that Q_A = 0.595 mm = 0.0595 cm. The calculated area of specimen LRM 1 is 1.88 cm^2, and the relative uncertainty in the area is 100 • (0.0595 cm^2/1.88 cm^2) = 3.16%.

The sample-to-sample variations in the surface roughness are assumed to be small because all specimens were prepared with the same surface finish. The uncertainty in the total surface area of disk-shaped specimens is taken to be 4% of the calculated area due to the combined effects of measurement and polishing.

B.2.2 Rectangular Specimens

The area of each parallelepiped specimen was calculated using the average of opposite side lengths (l is the average of l_1-$_2$ and $l_{3\text{-}4}$) and widths (w is the average of l_2-$_3$ and $l_{4\text{-}1}$,) and thicknesses (h is the average of the four corner thicknesses h_1, h_2, h_3, and h_4,). The total area is the area of the two faces plus the areas of the 4 sides, where opposite sides are assumed to have the same area (since they are based on the average length, width, and thickness):

$$A = 2 \bullet \left(\frac{l_{1-2} + l_{3-4}}{2} \bullet \frac{l_{2-3} + l_{4-1}}{2} \right) + 2 \bullet \left(\frac{l_{1-2} + l_{3-4}}{2} \bullet \frac{h_1 + h_2 + h_3 + h_4}{4} \right) + 2 \bullet \left(\frac{l_{2-3} + l_{4-1}}{2} \bullet \frac{h_1 + h_2 + h_3 + h_4}{4} \right). \quad \text{(B-5)}$$

$$A = 2 \bullet (l \bullet w) + 2 \bullet (l \bullet h) + 2 \bullet (w \bullet h). \quad \text{(B-6)}$$

Applying Equation B-1 to the area calculated with Equation B-6 gives

$$Q_{A_{side}}{}^2 = (2w + 2h)^2 \bullet q_l{}^2 + (2l + 2h)^2 \bullet q_w{}^2 + (2l + 2w)^2 \bullet q_h{}^2. \quad \text{(B-7)}$$

All dimensions were measured to ±0.0005 inches (0.013 mm), so that $q_l = q_w = q_t$ = 0.0005 in. (0.013 mm). Specimen LRM 14 has side lengths $l_{1\text{-}2}$= 0.4025 in., $l_{2\text{-}3}$= 0.2205 in., $l_{3\text{-}4}$= 0.3950 in., and $l_{4\text{-}1}$= 0.2225 in. and corner thicknesses are h_1 = 0.0270 in., h_2 = 0.0290 in., h_3 = 0.0275 in., and h_4 = 0.0270 in. The average length is 0.3988 in., the average width is 0.2215 in., the average thickness is h = 0.0276 in., and the calculated area is 0.2109 in.^{2} (1.361 cm^2). Inserting the experimental values gives

$$Q_{A_{side}}{}^2 = (2 \bullet 0.2215 + 2 \bullet 0.0276)^2 \bullet (0.0005)^2 + (2 \bullet 0.3988 + 2 \bullet 0.0276)^2 \bullet (0.0005)^2 + (2 \bullet 0.3988 + 2 \bullet 0.2215)^2 \bullet (0.0005)^2 = 6.286 \times 10^{-7}. \quad \text{(B-8)}$$

The uncertainty in the calculated area is Q_A = 7.93 x 10^{-4} in.^{2} (= 5.12 x 10^{-3} cm^2). The relative uncertainty in the area is 100 • (0.00512 cm^2/1.36 cm^2) = 0.376%.

The sample-to-sample variations in the surface roughness are assumed to be small because all specimens were prepared with the same surface finish. The uncertainty in the total surface area of parallelepiped-shaped specimens is taken to be 1% of the calculated area due to the combined effects of measurement and polishing.

B.3 SOLUTION VOLUME

The amounts of leachant solution added to the tests and the amounts of nitric acid solution in the acid strip analyses were determined by mass. The solution submitted for analysis was not otherwise diluted, and the dilution due to nitric acid is negligible. Only the uncertainty in the leachant mass is considered. The uncertainty in mass due to the difference in two mass measurements is used as the uncertainty in volume

by presuming a solution density of 1.00 g/mL for all test solutions. The masses were measured to the nearest 0.01 g, which is taken to be the measurement uncertainty. The solution mass was calculated as the difference between the mass of the test vessel or leachate sample bottle without solution and the mass of the vessel or bottle with the added solution. The uncertainty in the mass determination is calculated using propagation of errors formula in Equation B-1 for the equation M = $mass_1$ – $mass_2$ is as follows:

$$Q_M{}^2 = (\frac{\partial M}{\partial M_{mass\ 1}})^2 \bullet q_1{}^2 + (\frac{\partial M}{\partial M_{mass\ 2}})^2 \bullet q_2{}^2 . \quad \text{(B-9)}$$

If the uncertainty in each measured mass is $q_1 = q_2 = 0.01$ g, then

$$\frac{\partial M}{\partial mass_1} = 1 \quad \text{(B-10)}$$

$$\frac{\partial M}{\partial mass_2} = -1 \quad \text{(B-11)}$$

Inserting the experimental values gives

$$Q_M{}^2 = (1)^2 \cdot (0.01)^2 + (-1)^2 \cdot (0.01)^2 = 0.0002 . \quad \text{(B-12)}$$

The uncertainty in the difference of two masses is estimated to be $q_M = (0.0002)^{0.5} = 0.014$ g. The uncertainty in volume is estimated to be 0.014 mL. Tests were conducted with between about 30 and 60 g of water, and the relative uncertainties in these mass measurements range between 0.05% and 0.1%. The uncertainty in the volume is taken to be 0.02 mL for all tests.

$$q_V = 0.02\ mL . \quad \text{(B-13)}$$

B.4 SOLUTION CONCENTRATIONS

The uncertainties in the measured concentrations of all analytes were estimated by the ICP-MS analyst to be 10% of the measured values:

$$q_C = 0.1 \times C(i) . \quad \text{(B-14)}$$

B.5 NL(Si) IN IMMERSION TESTS

The uncertainty in the value of NL(Si) is due to uncertainties in the measured solution concentration, the specimen surface area, the solution volume, and the mass fraction of Si in the glass. The uncertainty in NL(Si) is determined by propagation of errors and applying Equation B-1 to the function given in Equation 1. Equation 1 is rewritten in terms of measured values as:

$$NL(Si) = \frac{\left(C(Si)_{test\ solution} - C°(Si)\right) \bullet V_{test\ solution}}{S \bullet f(Si)} . \quad \text{(B-15)}$$

Differentiating Equation B-15 gives the following terms:

$$Q_{C(Si)\_test\ solution} = \frac{\partial NL}{\partial C(Si)_{test\ solution}} = \frac{V_{test\ solution}}{S \times f(Si)} \quad \text{(B-16)}$$

$$Q_{C°(Si)} = \frac{\partial NL}{\partial C°(Si)} = \frac{-V_{test\ solution}}{S \times f(Si)} \tag{B-17}$$

$$Q_{V\_test\ solution} = \frac{\partial NL}{\partial V_{test\ solution}} = \frac{C(Si)_{test\ solution} - C°(Si)}{S \times f(Si)} \tag{B-18}$$

$$Q_S = \frac{\partial NL}{\partial S} = \frac{-\left(C(Si)_{test\ solution} - C°(Si)\right) \times V_{test\ solution}}{S^2 \times f(Si)} \tag{B-19}$$

$$Q_{f(Si)} = \frac{\partial NL}{\partial f(Si)} = \frac{-\left(C(Si)_{test\ solution} - C°(Si)\right) \times V_{test\ solution}}{S \times f(Si)^2} \tag{B-20}$$

In the form of Equation 1, the propagation expression is

$$Q_{NL}{}^2 = (Q_C)^2 \bullet q_C{}^2 + (Q_{C°})^2 \bullet q_{C°}{}^2 + (Q_V)^2 \bullet q_V{}^2 + (Q_S)^2 \bullet q_S{}^2 + (Q_{f\,(Si)})^2 \bullet q_{f(Si)}{}^2 + \tag{B-21}$$

where the q_x values give the analytical uncertainties for each measured parameter. As a sample calculation, for test LRM-1:

$C_{test\ solution}$ *(Si)* = 808 µg/L (8.08 x 10^{-4} g/L) with an uncertainty of 10%, (q_C = 8.08 x 10^{-5} g/L)
C°(Si) = 29 µg/L (2.90 x 10^{-5} g/L) with an uncertainty of 10%, ($q_{C°}$ = 2.90 x 10^{-6} g/L)
$V_{test\ solution}$ = 104.5 mL (0.1045 L) with uncertainty of 0.02 mL (q_V = 0.00002 L)
S = 1.88 cm^2 with an uncertainty of 4% (q_S = 0.0753 cm^2 = 7.53 x 10^{-6} m^2)
f(Si) = 0.2533 with an uncertainty of 0.0057 (q_f = 0.0057).

Inserting the experimental values for the partial derivatives with respect to *C, C°, V, S,* and *f(Si)* gives

$$Q_C = \frac{V}{(S \bullet f)} = 2193\,;\ Q_{C°} = \frac{-V}{(S \bullet f)} = -2193\,;\ Q_V = \frac{(C - C°)}{(S \bullet f)} = 16.34\,;\ Q_S = \frac{-(C - C°) \bullet V}{(S^2 \bullet f)} = -9080\,;\ \text{and}$$
$$Q_f = \frac{-(C - C°) \bullet V}{(S \bullet f^2)} = -6.745 \tag{B-22}$$

Inserting these values and the uncertainties into Equation B-21 gives

$$Q_{NL}{}^2 = (2193)^2 \bullet \left(8.08 \times 10^{-5}\right)^2 + (-2190)^2 \bullet \left(2.90 \times 10^{-6}\right)^2 + (16.34)^2 \bullet (0.00002)^2 + (-9080)^2 \bullet \left(7.53 \times 10^{-6}\right)^2 + (-6.745)^2 \bullet (0.0057)^2 = 0.0376\left(g/m^2\right)^2 \tag{B-23}$$

The uncertainty is Q_{NL} = $(0.0376)^{0.5}$ = 0.194 g/m^2. The calculated value of NL(Si) for this test is 1.71 g/m^2, and the relative uncertainty in NL(Si) is 100 • (0.194 g/m^2/1.71 g/m^2) = 11.3%.

The propagated uncertainties are summarized in Table B-1. The uncertainty in the normalized Si mass loss is dominated by the uncertainty in the measure concentrations of the test solutions. The variance in the surface area (Q_S^2 x q_S^2) contributes about 13% to the variance in NL(Si) for tests with disk-shaped specimens but only about 1% for tests with parallelepiped-shaped specimens.

B.7 TIME

The test duration is determined by the time between when the test vessel was placed in the oven and when it was removed from the oven, typically to the nearest 5 minutes. The time required for the solution and glass to heat from room temperature to the test temperature is not known, but is estimated to be the same for all tests at that temperature. The uncertainty in test duration is estimated to be 10 minutes (0.007 days). The uncertainty in the reaction is not propagated with the other test variables. In the plots and calculations, the reaction times are considered to the nearest 0.01 days. The uncertainty in the test time is negligible.

Table B-1. Propagation of Uncertainty for MCC-1 Tests

Test Number	$Q_V^2 * q_v^2$	$Q_C^2 * q_v^2$	$Q_{C^o}^2 * q_{C^o}^2$	$Q_S^2 * q_S^2$	$Q_{f(Si)}^2 * q_f^2$	Q_{NL}^2	Q_{NL}, g/m^2	NL/Q_{NL}
Series 1: Specimens with a 600 grit finish								
LRM-1	1.07E-07	3.14E-02	4.05E-05	4.67E-03	1.48E-03	3.76E-02	0.194	11.3%
LRM-2	1.03E-07	2.99E-02	4.05E-05	4.45E-03	1.41E-03	3.58E-02	0.189	11.4%
LRM-3	1.87E-07	5.93E-02	4.05E-05	8.99E-03	2.85E-03	7.12E-02	0.267	11.3%
LRM-4	2.43E-07	6.81E-02	4.05E-05	1.04E-02	3.28E-03	8.18E-02	0.286	11.2%
LRM-5	3.99E-07	1.17E-01	4.05E-05	1.80E-02	5.71E-03	1.41E-01	0.375	11.2%
LRM-6	1.50E-06	4.21E-01	4.05E-05	6.61E-02	2.09E-02	5.09E-01	0.713	11.1%
LRM-7	7.63E-07	2.04E-01	4.05E-05	3.17E-02	1.00E-02	2.46E-01	0.496	11.1%
LRM-8	7.33E-07	2.08E-01	4.05E-05	3.24E-02	1.02E-02	2.51E-01	0.501	11.1%
LRM-9	1.33E-06	3.35E-01	4.05E-05	5.25E-02	1.66E-02	4.04E-01	0.636	11.1%
LRM-10	1.41E-06	3.85E-01	4.05E-05	6.04E-02	1.91E-02	4.65E-01	0.682	11.1%
LRM-11	2.04E-06	5.27E-01	4.05E-05	8.29E-02	2.62E-02	6.36E-01	0.798	11.1%
LRM-12	3.90E-06	1.05E+00	4.05E-05	1.66E-01	5.27E-02	1.27E+00	1.128	11.1%
LRM-13	3.61E-06	1.06E+00	4.05E-05	1.67E-01	5.29E-02	1.28E+00	1.131	11.1%
Series 2: Specimens with a 800 grit finish								
LRM-14	1.41E-07	2.08E-02	6.81E-06	2.01E-04	1.02E-03	2.21E-02	0.149	10.5%
LRM-15	4.67E-08	1.27E-02	6.81E-06	1.21E-04	6.12E-04	1.34E-02	0.116	10.5%
LRM-16	2.68E-07	3.89E-02	6.81E-06	3.79E-04	1.92E-03	4.12E-02	0.203	10.4%
LRM-17	1.32E-07	3.55E-02	6.81E-06	3.45E-04	1.75E-03	3.76E-02	0.194	10.4%
LRM-18	9.95E-07	1.39E-01	6.81E-06	1.37E-03	6.94E-03	1.47E-01	0.384	10.4%
LRM-19	1.51E-06	2.20E-01	6.81E-06	2.18E-03	1.10E-02	2.34E-01	0.483	10.4%
LRM-20	6.08E-06	8.57E-01	6.81E-06	8.52E-03	4.31E-02	9.08E-01	0.953	10.3%
LRM-21	1.92E-06	4.89E-01	6.81E-06	4.86E-03	2.46E-02	5.19E-01	0.720	10.3%
LRM-22	1.07E-06	2.86E-01	6.81E-06	2.84E-03	1.44E-02	3.04E-01	0.551	10.3%
LRM-23	1.92E-05	1.73E+00	6.81E-06	1.72E-02	8.71E-02	1.83E+00	1.353	10.3%
Series 3: Specimens with a 1200 grit finish								
LRM-24	7.20E-08	9.65E-03	1.56E-06	9.41E-05	4.77E-04	1.02E-02	0.101	10.4%
LRM-25	6.24E-08	8.65E-03	1.56E-06	8.42E-05	4.26E-04	9.16E-03	0.096	10.4%
LRM-26	2.95E-07	4.05E-02	1.56E-06	3.99E-04	2.02E-03	4.29E-02	0.207	10.4%
LRM-27	2.29E-07	5.82E-02	1.56E-06	5.76E-04	2.92E-03	6.17E-02	0.248	10.3%
LRM-28	1.33E-06	1.87E-01	1.56E-06	1.86E-03	9.40E-03	1.98E-01	0.445	10.3%
LRM-29	1.54E-06	3.96E-01	1.56E-06	3.95E-03	2.00E-02	4.20E-01	0.648	10.3%
LRM-30	2.63E-06	3.56E-01	1.56E-06	3.54E-03	1.79E-02	3.77E-01	0.614	10.3%
LRM-31	1.20E-06	2.93E-01	1.56E-06	2.92E-03	1.48E-02	3.11E-01	0.558	10.3%
LRM-32	1.14E-06	9.84E-02	1.56E-06	9.76E-04	4.94E-03	1.04E-01	0.323	10.3%
LRM-33	5.45E-06	7.17E-01	1.56E-06	7.15E-03	3.62E-02	7.60E-01	0.872	10.3%
LRM-34	6.59E-06	8.73E-01	1.56E-06	8.71E-03	4.41E-02	9.26E-01	0.962	10.3%
LRM-35	8.33E-06	1.15E+00	1.56E-06	1.14E-02	5.79E-02	1.21E+00	1.102	10.3%

Distribution for ANL/06-51

Internal (Printed and Electronic Copies):

W. L. Ebert (10)

Internal (Electronic Copy Only):

A. J. Bakel
D. B. Chamberlain
J. C. Cunnane
J. A. Fortner
D. J. Graziano
J. L. Jerden, Jr.
M. C. Regalbuto
V. S. Sullivan
Y. Tsai

External (Electronic Copies Only):
M. A. Buckley, ANL Library-E
R. Blauvelt, Navarro, Inc., Middletown, OH
K. Chun, Korea Atomic Energy Research Institute, Yuseong, Daejon, Republic of Korea
S. M. Frank, Idaho National Laboratory, Idaho Falls, ID
P. Fugier, Commissariat à l' énergie atomique, Valrhô Marcoule, France
S. Gin, Commissariat à l' énergie atomique, Valrhô Marcoule, France
B. D. Hanson, Pacific Northwest National Laboratory, Richland, WA
V. J. Jain, Center for Nuclear Waste Regulatory Analyses, San Antonio, TX
C. M. Jantzen, Savannah River National Laboratory, Aiken, SC
S. Kim, Korea Atomic Energy Research Institute, Yuseong, Daejon, Republic of Korea
J. C. Marra, Savannah River National Laboratory, Aiken, SC
L. Niemann, Forschungszentrum Karlsruhe, Karlsruhe, Germany
T. P. O'Holleran, Idaho National Laboratory, Idaho Falls, ID
E. M. Pierce, Pacific Northwest National Laboratory, Richland, WA
K. Satake, JNC Tokai Works, Ibaraki, Japan
G. L. Smith, Pacific Northwest National Laboratory, Richland, WA
D. M. Strachan, Pacific Northwest National Laboratory, Richland, WA
C. Veyer, Saint Waast la Valleé, France
H. Yoshikawa, JNC Tokai Works, Ibaraki, Japan

Chemical Engineering Division
Argonne National Laboratory
9700 South Cass Avenue, Bldg. 205
Argonne, IL 60439-4837

www.anl.gov

UChicago ▶ Argonne LLC

A U.S. Department of Energy laboratory
managed by UChicago Argonne, LLC